Brazilian Journal of Probability and Statistics
2009, Vol. 23, No. 2, 166–178
DOI: 10.1214/00-BJPS020

Markovian classification of SAR images using $\mathcal{G}_I^0$ model

Mery Picco and Gabriela Palacio
Universidad Nacional de Río Cuarto

Abstract. When processing synthetic aperture radar (SAR) images, there is a strong need for statistical models of scattering to take into account multiplicative noise. For instance, the classification process needs to be based on the use of statistics. Our main contribution is the choice of an accurate model for SAR images over urban areas and its use in a Markovian classification algorithm. Clutter in SAR images becomes non-Gaussian when the resolution is high or when the area is manmade. Many models have been proposed to fit with non-Gaussian scattering statistics (K, Weibull, Log-normal, etc.), but none of them is flexible enough to model all kinds of surfaces. Frery et al. [*IEEE Transactions on Geoscience and Remote Sensing* **35** (1997) 648–659] proposed a new class of distributions, $\mathcal{G}$ distribution, arising from the multiplicative model. Classical distributions such as $\mathcal{K}$ are particular cases of this new class. A special case of this class called $\mathcal{G}^0$ is shown able to model extremely heterogeneous clutter, such as that of urban areas. The quality of the classification obtained by mixing this model and a Markovian segmentation is high.

1 Introduction

Classification of land cover is one of the primary objectives in the remotely sensed data analysis. In synthetic aperture radar (SAR) data, the accuracy of pixel-based classifiers is affected by a fading effect called speckle, which manifests itself as a strong granularity in detected images. To combat the effect of speckle on the pixel-based classifiers, neighborhood, or contextual information is often incorporated into the classification methodology. Markov Random Fields (MRF) are frequently employed to model neighborhood and class label structure for the classification of remotely sensed data. Using MRF models in the classification of SAR data allows us to obtain better results than non-contextual classification methods (Solberg, Taxt and Jain (1996); Vieira (1996)). The MRF-based classifier requires: (1) to choose a suitable model to the observed image, (2) to incorporate the a priori spatial information, and (3) to obtain an initial class image. In relation to the first point, there exist many different models for SAR images, such as K (Jakeman and Pusey (1976); Oliver (1984)), Beta (Lopes, Laur and Nezry (1990)), Weibull (Menon (1963); Oliver (1993)), and Nakagami–Rice (Dana and Knepp (1986)).

Key words and phrases. Classification, Markovian segmentation, statistical model, synthetic aperture radar (SAR), urban areas.
Received August 2008; accepted December 2008.

None of them provide a good solution, mainly because they do not have a sufficiently large field of applications. Tison et al. (2004) proposed the Fisher model for high-resolution SAR images over urban areas. They obtained excellent results in classification. In order to take into account the entire diversity of the scene, Frery et al. (1997) proposed the Γ^{-1} and $\Gamma^{-1/2}$ distributions for the intensity (X) and amplitude ($\sqrt{X}$) backscatter, respectively. These new models, when used alongside the classical one for the speckle noise, yield new distributions for the return, called $\mathcal{G}_I^0$ and $\mathcal{G}_A^0$. The advantage of these distributions is that they model not only extremely heterogeneous areas, such as cities, but also moderately heterogeneous areas such us forests, or homogeneous areas such us pastures. The $\mathcal{K}$ distribution fails to model many situations where the return is extremely heterogeneous (Mejail et al. (2001); Müller et al. (2000)).

Moreover, as the ground data can be characterized by the $\mathcal{G}_I^0$ parameters, their estimation for each pixel may lead to estimated parameter maps that, in turn, can be used as the input for a non-contextual classification method. Using these ideas and $\mathcal{G}_A^0$ distribution (for amplitude image), Mejail et al. (2003) showed that this classification scheme produces better results than a classical method (Lee filter and Gaussian classification).

Based on these results, we propose a MRF-based classification scheme for intensity images that uses the $\mathcal{G}_I^0$ distribution to model the observed image and the estimated parameter maps to obtain an initial class image. We hope to achieve a classification algorithm more efficient than the one proposed by Mejail et al. (2003) by using a suitable model for the observed data in a Bayesian classification scheme and incorporate the spatial context in a Markovian framework. The classification process is described in Section 4. The full process has been tested on real and simulated radar images. The results are presented in Section 5, and a critical discussion of results and methodology concludes the paper (see Section 6).

2 The multiplicative model

Only univariate signals will be discussed here. Any reader interested in multivariate SAR statistical modeling may refer to Freitas, Frery and Correia (2005).

Goodman (1985) provided one of the first rigorous statistical frameworks, known as the "Multiplicative Model", for dealing with speckle noise in the context of laser imaging. The use of such a framework has led to the most successful techniques for SAR data processing and analysis. This phenomenological model states that the observation in every pixel is the outcome of a random variable $Z : \Omega \to \mathbb{R}^+$ that, in turn, is the product of two independent random variables: $X : \Omega \to \mathbb{R}^+$, the ground truth or backscatter, related to the intrinsic dielectric properties of the target, and $Y : \Omega \to \mathbb{R}^+$, the speckle noise, obeying a unitary mean Gamma law. The distribution of the return, $Z = XY$, is completely specified by the distributions of X and Y. The univariate multiplicative model began as a single distribution, namely the Rayleigh law, was extended by Yueh et al. (1989) to accomodate

the $\mathcal{K}$ law, and later improved further by Frery et al. (1997) to the $\mathcal{G}$ distribution that generalizes all the previous probability distributions. The density function that describes the behavior of the speckle noise in intensity images is $\Gamma(L; L)$, where L is the number of looks, a parameter related to the visual quality of the image that can be controlled to a certain extent during the generation of the data.

The most successful models for the backscatter are particular cases of the generalized inverse Gaussian distribution (Frery et al. (1997)), being the main ones a constant (c), the Gamma $\Gamma(\alpha, \lambda)$, Reciprocal of Gamma $\Gamma^{-1}(\alpha, \gamma)$ and Inverse Gaussian $IG(\omega, \sigma)$ laws (for the last one see Müller et al. (2000)). These models for the backscatter yield the following distributions for the return Z, respectively: $\Gamma(L, L/c)$, $\mathcal{K}(\alpha, \lambda, L)$, $\mathcal{G}_I^0(\alpha, \gamma, L)$, and $\mathcal{G}_I^H(\omega, \sigma, L)$ (for more details see Moschetti et al. (2006)). Müller et al. (2000) showed that the last two models are more appropriate for areas with different degrees of heterogeneity. Mejail et al. (2003) obtained excellent results using the analogous model ($\mathcal{G}_A^0$) for the amplitude return.

3 Supervised statistical classification

A classification process transforms the original image into another one of the same size in which the value of each pixel is a label that identifies the assigned category to this pixel, that is, data are transformed into thematic information. In a supervised classification, the identity and location of specific sites in the image that represent homogeneous examples of land-cover types are a priori known. These areas are called training sites because their spectral characteristics are used to train the classification algorithm for eventual land-cover mapping of the remainder of the image (Jensen (2005)). Maximum likelihood Gaussian (MLG) is the most widely used supervised classification algorithm. This algorithm assumes that the training data statistics for each class are normally distributed (Gaussian) and each class is characterized by the value of their parameters. The MLG rule calculates the probability of a pixel belonging to each of m classes and assigns each pixel to the class of highest probability. This algorithm classifies each pixel individually without taking into account the contextual information. However, neighboring pixels tend to have similar class labels. For example, if a pixel has label sky, there is high probability that the neighboring pixels also have the same label. Modeling this dependence is crucial to achieve good classification accuracy. MRF-based classification methods incorporate this spatial dependence and therefore have been successfully used in image restoration (Bustos, Frery and Ojeda (1998); Carnevalli, Coletti and Patarnello (1985); Geman and Geman (1984); Winkler (2006)).

3.1 Classification based on Markov random fields

Let $\mathbf{Z} = (Z_s)_{s \in S}$ be the observed image and $\mathbf{L} = (L_s)_{s \in S}$ the unknown class image. Here, we suppose that the random variables $\mathbf{Z} = (Z_s)_{s \in S}$ are conditionally

independent with respect to $\mathbf{L}$ and that the distribution of each Z_s conditional on $\mathbf{L}$ is equal to its distribution conditional on L_s. The restoration method proposed by Geman and Geman (1984) assumes that the a priori distribution of $\mathbf{L}$ can be modeled by a Markov process, that is,

$$P\big(L_s = l_s/(L_t = l_t)_{t\in S, t\neq s}\big) = P\big(L_s = l_s/(L_t = l_t)_{t\in V_s}\big), \tag{3.1}$$

where V_s denote a neighborhood of the pixel s, that is, the probability that the pixel s belongs to a certain class l_s conditional on the classes attributed to the pixels in the rest of the image is equal to the probability of l_s conditional on the classes of the pixels in the neighborhood V_s.

Bayes' rule and the Hammersley–Clifford theorem allow us to write the a posteriori probability as

$$P(\mathbf{L} = \mathbf{l}/\mathbf{Z} = \mathbf{z}) = \frac{1}{W}\exp\Big(\sum_{s\in S}\log f_{l_s}, (z_s) - U(l)\Big), \tag{3.2}$$

where W is a normalizing factor, the first term inside the exponential function is the component of MLG algorithm, and the second one is the component of the context, which measures the influence of neighboring classes.

The objective is, given an image $\mathbf{Z}$, to determine the configuration $\mathbf{L}$ that maximizes (3.2). Since the space of configurations is too large it is not possible to determine $\mathbf{L}$ directly. Metropolis and Gibbs sampler algorithms allow us to obtain realizations of $\mathbf{L}$ from local characteristics of the field

$$\begin{aligned} &P\big(L_s = l_s/Z_s = z_s, (L_t = l_t)_{t\in V_s}\big) \\ &\quad = \frac{1}{W'_s}\exp\big(-U_s(l_s, (l_t)_{t\in V_s}) + \log f_{l_s}(z_s)\big). \end{aligned} \tag{3.3}$$

For simplicity, we restrict our attention to the Potts model, four-connectivity and cliques of type C_2 (Winkler (2006)), where $U_s(l_s, (l_t)_{t\in V_s})$ represents the number of pixels $t \in V_s$ for which $l_t \neq l_s$ minus the number of pixels for which $l_t = l_s$, multiplied by a regularity parameter λ.

In this work we will use the Gibbs sampler algorithm with decreasing temperature (simulated annealing).

4 Algorithm of classification proposed

Classification methods based on Markov Random Fields require an initial class image, the knowledge of the density of the observed image conditional on the class image and a probability measure in the configuration space (a priori distribution). Classically, the initial image is the result of k-means algorithm or MLG. Generally the k-means class image is very irregular due to the speckle (Fjortoft et al. (2003)), while the MLG one is of low quality, since the Gaussian model is not

suitable to SAR images. Frery et al. (1997) proposed the $\mathcal{G}_A^0$ distribution showing it is a good model for SAR amplitude images. Since the ground data can be characterized by the parameters α and γ, their estimation for each pixel may lead to estimated parameter maps that, in turn, can be used as the input for classification methods, among other applications. Using these ideas and the $\mathcal{G}_A^0$ distribution Mejail et al. (2003) proposed a classification scheme for amplitude images based on feature extraction, followed by MLG classification, obtaining very good results. The algorithm proceeds as follows:

- Obtain the $\hat{\alpha}$ and $\hat{\gamma}$ images using a 7×7 sliding window and replace the value of the central pixel with the estimation of the corresponding parameter ($\mathcal{G}_A^0$ distribution).
- Use the $\hat{\alpha}$ and $\hat{\gamma}$ images as inputs for a MLG method.

Although this algorithm outperforms the results obtained with a classical scheme (Lee filter and Gaussian classification), it does not take into account the contextual information. Moreover, the parameter estimations may be affected by the presence of pixels of different classes and hence the resulting value does not represent the ground truth.

In this paper, we propose a classification scheme which aims to take the advantages of the algorithm proposed by Mejail et al. (2003) improving its performance by incorporating the contextual information. This classification method includes the following steps:

- We start from initial class image L^0 obtained as Mejail et al. (2003) (using $\mathcal{G}_I^0$ distribution).
- We sweep the image repeatedly until convergence. For each iteration q and for each pixel s:

  (a) the local a posteriori distribution given by (3.2) is computed;

  (b) the pixel is attributed to a class randomly drawn according to this distribution in the following way: we consider the interval [0, 1] and we attribute to each class a subinterval where the width is equal to the probability of this class. A uniformly distributed random number in [0, 1] is generated, and the class is selected according to the subinterval in which this random number falls.

To evaluate the performance of the proposed methodology, the following four classification methods will be compared:

- M1: Lee-filtered data classified with Gaussian maximum likelihood (classical method).
- M2: $(\hat{\alpha}, \hat{\gamma})$ data classified with Gaussian maximum likelihood (the algorithm proposed by Mejail et al. (2003)).
- M3: Markovian classification using the result of M1 algorithm as initial class image (classical MRF-based method).

- M4: Markovian classification using the result of M2 algorithm as initial class image (algorithm proposed in this paper).

In order to ensure fair treatment of all algorithms, the majority-filter was applied using a 11×11 window. For the Lee filter 7×7 windows size are used.

Samples from the training areas were taken to estimate the mean and the standard deviation of each class, used to determine the MLG classification rule, and $\mathcal{G}_I^0$ parameters, used for MRF-based classification methods.

To estimate the parameters of the $\mathcal{G}_I^0$ distribution several techniques are available, the most remarkable ones being those based on maximum likelihood or on sample moments.

To estimate the α and γ parameters it is necessary, then, to estimate two moments. In this work moments of order $1/2$ and 1, namely $m_{1/2}$ and m_1 respectively, will be used. These moments can be obtained of the following equation:

$$E(Z^r) = \frac{\Gamma(-\alpha - r)\Gamma(L + r)}{\Gamma(-\alpha)\Gamma(L)} \left(\frac{\gamma}{L}\right)^r, \tag{4.1}$$

if $r < -2\alpha$. These estimators are also used to get the $\hat{\alpha}$ and $\hat{\gamma}$ images.

In our experience with simulated images (with different values of the parameters and different seeds) we observed that the estimated value of α based on $m_{1/2}$ and m_1 moments is close to the truth value, except when the area is homogeneous. In this case, in approximately 40 percent of the times no estimated value is available (2 percent in heterogeneous areas) while approximately 40 percent of the times the estimation corresponds to a different type of area (5 percent in heterogeneous areas). Hence, in homogeneous areas only 20 percent of the times the area is correctly identified, while in heterogeneous areas this occurs in 93 percent of times.

For this reason we decided to set $\hat{\alpha} = -20$ when the estimation is not available, rather than the median of the observed estimations in a window around the pixel (as proposed by Mejail et al. (2003)).

5 Data analysis

One of the most important ways to assess the adequacy of a theory to reality, in this context, is the use of stochastic simulation. In the following, an experiment involving simulation and estimation will be shown. This simulated image will be used to test the performance of the classification procedures described above. Before the simulated example is presented, one real SAR image will be classified with the $\mathcal{G}_I^0$ model and the proposed methodology.

To quantify the quality of the classification the confusion matrix is commonly used. However, the overall analysis of their cells is difficult, in particular when the image has several classes and we want to compare several classification methods.

From the confusion matrix X, the estimated Kappa coefficient of agreement can be calculated

$$\hat{\kappa} = \frac{X_{\bullet\bullet} \sum_k X_{kk} - \sum_k X_{k\bullet} X_{\bullet k}}{(X_{\bullet\bullet}^2) - \sum_k X_{k\bullet} X_{\bullet k}}. \tag{5.1}$$

A $\hat{\kappa}$ value close to one indicates agreement between the map and the truth, while values close to zero suggest the observed agreement is due to randomness.

For simulated images, the validation is made with the entire image, whereas for real images only a learning pixel set is used (Agresti (1990); Chuvieco (2002)).

5.1 Real image

Figure 1 shows an 370 × 370 extract of an ERS-2 three-look intensity image obtained in 1997 over the city of Cordoba (−31.3; −63.7), Argentina, with the training areas marked. By prior knowledge of the area, it was decided to classify the image into three classes. Figure 2 shows the initial classifications obtained with M1 and M2 algorithms. In the first one, a high level of confusion exists between the downtown area and suburb area (due to the low level of contrast between them), and its Kappa coefficient is very low (0.512). In the second one, this value rises to 0.812. These results are consistent with those obtained by Mejail et al. (2003) for amplitude images. Table 1 shows the estimated values of Kappa for M3 and M4 methods corresponding to different number of iterations. These results suggest that incorporating the contextual information in Bayesian framework improves the

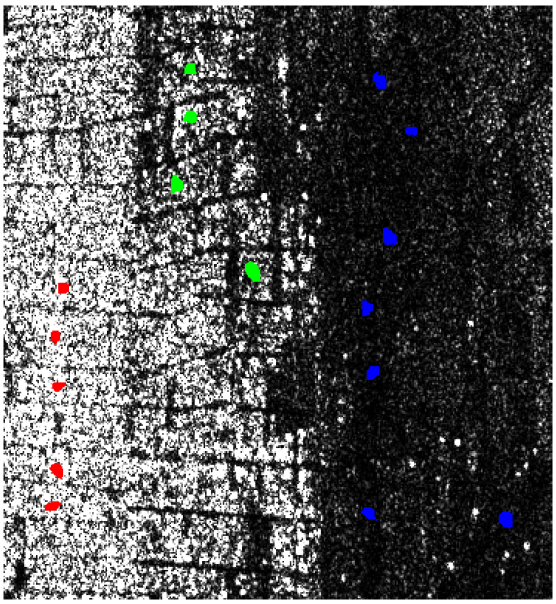

Figure 1 *Intensity image of Cordoba (Argentina), showing the training areas as colored spots.*

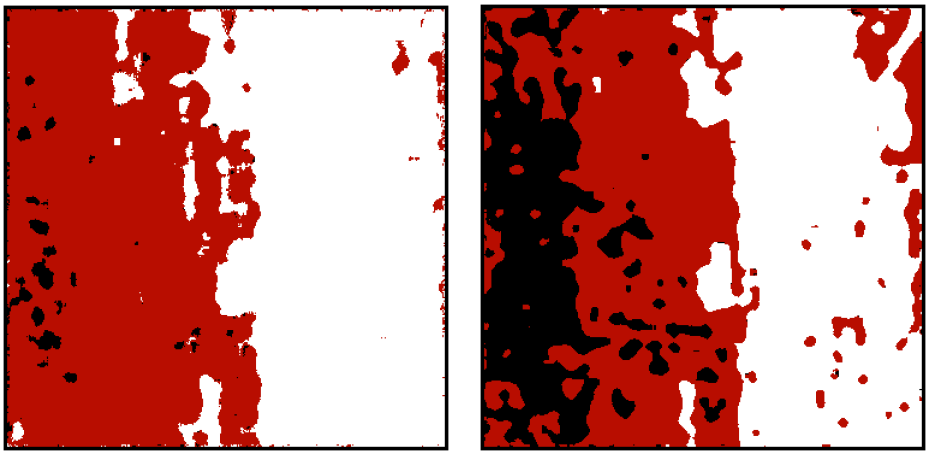

(a) (b)

Figure 2 (a) *Gaussian maximum classification of the Lee-filtered image.* (b) *Gaussian maximum likelihood classification of the* $\hat{\alpha}$ *and* $\hat{\gamma}$ *image.*

Table 1 *Kappa coefficient for Markovian classification methods (real image)*

	Number of iterations		
Method	10	100	300
M3	0.518	0.745	0.945
M4	0.962	0.962	0.947

classification quality. We observed that M4 method attains a Kappa coefficient of 0.962 with 10 iterations, while the M3 algorithm requires 300 iterations to achieve a similar value of Kappa. We observed that M4 reduces slowly its Kappa coefficient when the number of iterations increases from 100 to 300, whereas one would expect a higher value. This happens because the Kappa coefficient is estimated from one sample; nevertheless a confidence interval shows that the difference between them is not statistically significant.

Figure 3 shows that the classification obtained with M4 is better than the one obtained by M3 (both with 100 iterations), which indicates that using the estimated parameter map as the input for a contextual classification method yields better results.

5.2 Simulated image

The step based on simulation employs a simulated image using pdfs deduced from the statistics of real data. Figure 4(a) and (b) represents an ideal class image with

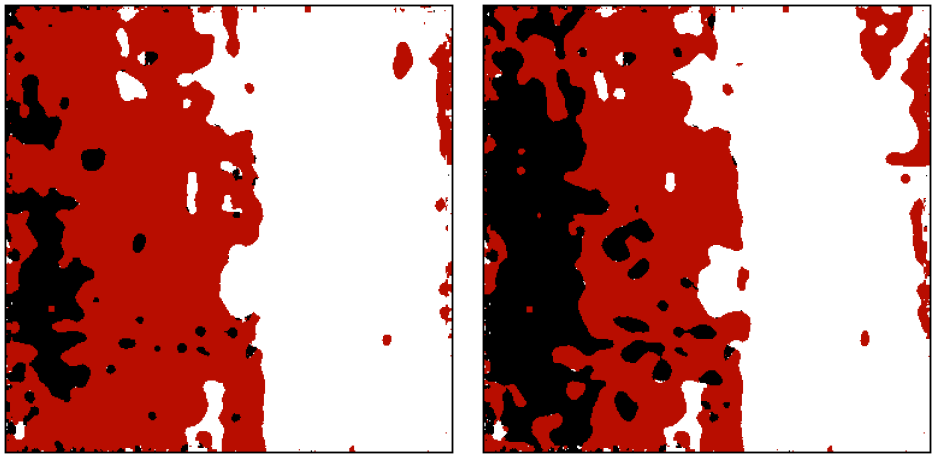

(a) (b)

Figure 3 *Result of Markovian classification using two initial class image* L^0*:* (a) *Gaussian maximum classification of the Lee-filtered image,* (b) *Gaussian maximum likelihood classification of the* $\hat{\alpha}$ *and* $\hat{\gamma}$ *image.*

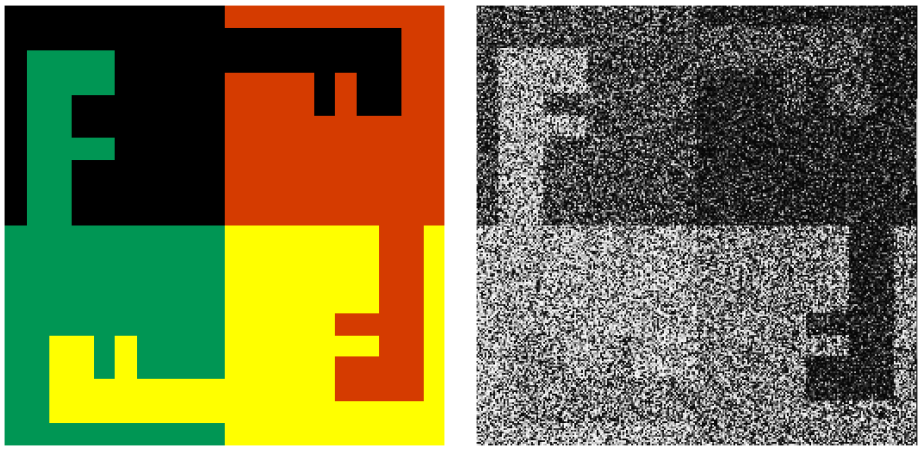

(a) (b)

Figure 4 (a) *Phantom with four classes.* (b) *Speckled image based on the four classes and* $\mathcal{G}_I^0$ *models for the return.*

four regions and its one-look speckled counterpart. The regions represent heterogeneous ($\alpha = -4$), homogeneous ($\alpha = -10$), and extremely heterogeneous ($\alpha = -2$, and $\alpha = -2.5$) areas. The values of γ are selected to obtain an image with low contrast between regions (as noted by Chuvieco (2002), when there are different areas with a similar reflectance, the non-contextual classification methods are not always able to separate them).

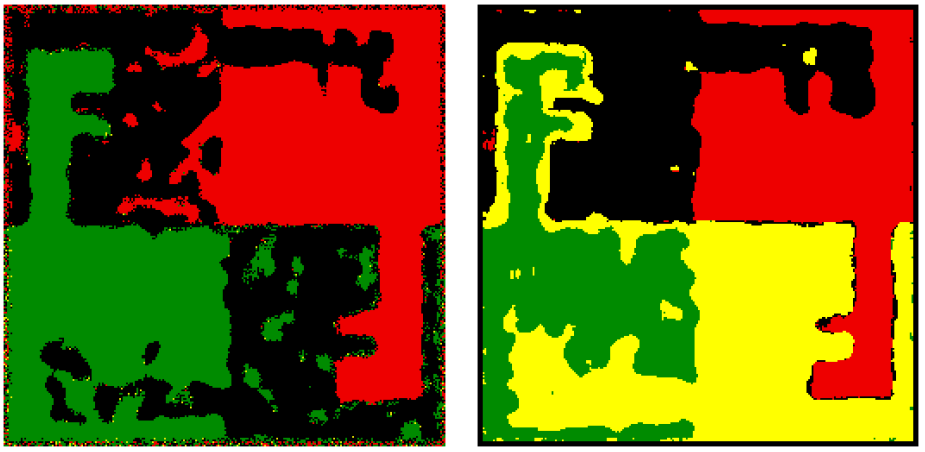

(a) (b)

Figure 5 (a) *Gaussian maximum classification of the Lee-filtered image.* (b) *Gaussian maximum likelihood classification of the* $\hat{\alpha}$ *and* $\hat{\gamma}$ *image.*

Table 2 *Kappa coefficient for Markovian classification methods (simulated image)*

	Number of iterations		
Method	10	100	300
M3	0.592	0.613	0.654
M4	0.884	0.912	0.921

The $L = 1$ case is chosen for this study since it corresponds to the noisiest class of intensity images, namely single look where no multilook processing has been performed. The M1 algorithm yields the map presented in Figure 5(a). This map is unacceptable in any practical application, since the mixture of yellow and black classes is too strong (yellow class disappears). The Kappa coefficient is 0.585. Figure 5(b) shows the result of applying M2 method. Visually, the classification result is far better than that given in Figure 5(a), and the Kappa coefficient, 0.867, is significantly better. Table 2 shows the estimated values of Kappa for M3 and M4 methods corresponding to a different number of iterations. We can conclude that the use of contextual information improves outcomes and that M4 significantly outperforms M3 [the classified images are shown in Figure 6(a) and 6(b), respectively].

(a) (b)

Figure 6 *Result of Markovian classification using two initial class image* L^0*:* (a) *Gaussian maximum classification of the Lee-filtered image,* (b) *Gaussian maximum likelihood classification of the* $\hat{\alpha}$ *and* $\hat{\gamma}$ *image.*

6 Conclusions

This paper has proposed a classification method based on Markovian random fields that requires a statistical model. Classical models are not accurate enough to model the diversity of the scenes. The use of the $\mathcal{G}_I^0$ distribution has several advantages over the more classical $\mathcal{K}$ law, from both the analytical and practical viewpoints. Their parameters have the same interpretation as those of the $\mathcal{K}$, with the advantage of being easier to estimate and able to explain extremely heterogeneous data. The estimation of its parameters, which is a simple computational task, allows the derivation of features that can be used in a classification scheme, getting better results than those produced by a traditional method (Lee filter and MLG classification rule). This result can be improved by incorporating the a priori spatial information in a Bayesian classification scheme.

We propose to use $\mathcal{G}_I^0$ distribution in two ways: first, to obtain an initial class image for MRF-based classification algorithm, and second, to model the distribution of the observed image (likelihood), which is required in a Bayesian classification scheme. The results obtained show that the incorporation of contextual information in a Markovian framework, and using an accurate model for observed image produce better results than using pixel-based classification rules.

References

Agresti, A. (1990). *Categorical Data Analysis*. Wiley, New York. MR1044993

Bustos, O. H., Frery, A. C. and Ojeda, S. (1998). Strong Markov processes in image modelling. *Brazilian Journal of Probability and Statistics* **12** 373–383. MR1718570

Carnevalli, P., Coletti, L. and Patarnello, S. (1985). Image processing by simulated annealing. *IBM Journal of Research and Development* **29** 569–579.

Chuvieco, E. (2002). *Teledetección Ambiental*. Editorial Ariel S. A., Barcelona.

Dana, R. and Knepp, D. (1986). The impact of strong scintillation on space based radar design ii: Noncoherent detection. *IEEE Transactions on Aerosp. Electron. Syst.* **AES-22** 34–46.

Fjortoft, R., Delignon, Y., Pieczynski, W., Sigelle, M. and Tupin, F. (2003). Unsupervised classification of radar images using hidden Markov chains and hidden Markov random fields. *IEEE Transactions on Geoscience and Remote Sensing* **41** 675–686.

Freitas, C. C., Frery, A. C. and Correia, A. H. (2005). The polarimetric G distribution for SAR data analysis. *Environmetrics* **16** 13–31. MR2146895

Frery, A. C., Müller, H. J., Yanasse, C. C. F. and Sant'Anna, S. J. S. (1997). A model for extremely heterogeneous clutter. *IEEE Transactions on Geoscience and Remote Sensing* **35** 648–659.

Geman, D. and Geman, S. (1984). Stochastic relaxation, Gibbs distributions and the Bayesian restoration of images. *IEEE Transactions on Pattern Analysis and Machine Intelligence* **6** 721–741.

Goodman, J. W. (1985). *Statistical Optics*. Wiley, New York.

Jakeman, E. and Pusey, N. (1976). A model for non Rayleigh sea echo. *IEEE Transactions on Antennas and Propagation* **AP-24** 806–814.

Jensen, J. R. (2005). *Introductory Digital Image Processing: A Remote Sensing Perspective*. Prentice Hall, New Jersey.

Lopes, A., Laur, H. and Nezry, E. (1990). Statistical distribution and texture in multilook and complex SAR images. In *Proc. IGARSS* 20–24.

Mejail, M. E., Frery, A. C., Jacobo-Berlles, J. and Bustos, O. (2001). Approximation of distributions for SAR images: Proposal, evaluation and practical consequences. *Latin American Applied Research* **31** 83–92.

Mejail, M. E., Jacobo-Berlles, J., Frery, A. C. and Bustos, O. H. (2003). Classification of SAR images using a general and tractable multiplicative model. *International Journal of Remote Sensing* **24** 3565–3582.

Menon, M. (1963). Estimation of the shape and scale parameters of the Weibull distribution. *Technometrics* **5** 175–182. MR0189173

Moschetti, E., Palacio, M. G., Picco, M. L., Bustos, O. and Frery, A. (2006). On Lee's protocol for speckle reduction techniques. *Latin American Applied Research* **36** 115–121.

Müller, H. J., Frery, A. C., Jacobo-Berlles, J., Mejail, M. and Moreira, J. R. (2000). The harmonic branch of the multilplicative model: Properties and application. In *EUSAR Proceedings VDE-Verlag* 301–310. München.

Oliver, C. (1984). A model for non-Rayleigh scattering statistics. *Opt. Acta* **31** 701–722.

Oliver, C. (1993). Optimum texture estimators for SAR clutter. *J. Phys. D: Appl. Phys.* **26** 1824–1835.

Solberg, A. H., Taxt, T. and Jain, A. K. (1996). A Markov random field model for classification of multisource satellite imagery. *IEEE Transactions on Geoscience and Remote Sensing* **34** 100–113.

Tison, C., Nicolas, J. M., Tupin, F. and Maître, H. (2004). A new statistical model for Markovian classification of urban areas in high-resolution sar images. *IEEE Transactions on Geoscience and Remote Sensing* **42** 2046–2057.

Vieira, P. R. (1996). Maximun likelihood and ICM SAR image classifiers. M.Sc. thesis, INPE, Brasil.

Winkler, G. (2006). *Image Analysis, Random Fields and Markov Chain Monte Carlo Methods: A Mathematical Introduction*. Springer, Berlin. MR1950762

Yueh, S. H., Kong, J. A., Jao, J. K., Shin, R. T. and Novak, L. M. (1989). K-distribution and polarimetric terrain radar clutter. *Journal of Electromagnetic Waves and Applications* **3** 747–768.

Universidad Nacional de Río Cuarto
Cuarto, Ruta Nac.
36-Km. 601-Código
Postal X5804BYA
Río Cuarto, Córdoba
Argentina
E-mail: mpicco@exa.unrc.edu.ar
gpalacio@exa.unrc.edu.ar